Pocklington equation method versus curved segments technique for the numerical study of circular antennas

J. Sosa-Pedroza, V. Barrera-Figueroa, J. López-Bonilla.
SEPI-ESIME-Zacatenco.
Instituto Politécnico Nacional.
Edif. Z-4, 3er. Piso, Col. Lindavista, CP 07738 México DF.
E-mail: jlopezb@ipn.mx

We present a mathematical model applying the general Pocklington equation to arbitrary shaped thin wire antennas. In order to simplify the antenna analysis this approach uses the point matching technique and a simplified kernel form. By means of this technique it is possible to increase the Method of Moments solution convergence and reduce computational time and effort. To exemplity this the procedure is applied to the well-known circular loop antenna. The obtained results are compared with those of Champagne method, which uses quadratic segments, in order to get a numerical solution for the Electric Field Integral Equation.

Keywords: *Curved segments, vector potential, Pocklington equation, method of moments.*

Introduction

Numerical analysis is a very common subject in many engineering disciplines; especially in antenna analysis and design which has developed widely thanks to computer technology. Many numerical codes, such as NEC, provide useful tools for antenna engineers. However, there is always the need to look into new techniques that bring forth the most convenient solution for a specific problem. Here we present a technique using Pocklington equation for arbitrary geometry thin wires [1] and including the simplification of the integral kernel. In order to get computational solution, once the integral equation has been established, the methodology requires to specify the antenna geometry by establishing vectorial equations for the wire axis and the equivalent current filament. Finally, general Pocklington equation is solved via Method of Moments (MM). As an example of this we present the solution for the current distribution of a circular loop antenna. The results are then compared with those obtained by Champagne et al [2], who apply Mei's procedure [3] of mixed potential integral equation and use at least three points to define a quadratic segment. Considering that Champagne's method uses 8 quadratic segments, each one of three points, we get a total of 17 points. We use the same number of points to get same results but now with the very simple technique of point matching and even with the simpler Simpson's rule for integration.

General Pocklington equation formulation

As it is known, Pocklington equation sets a relation between the current distribution in a straight wire and the impressed electric field on its surface. It is a classical model that considers an antenna made of a perfect conductor, of a small radius compared to the wave-length of the electromagnetic field. Pocklington approach assumes that the

current density in the surface conductor can be simulated by a current filament parallel to the antenna axis, leaving the rest of the conductor as part of the free space as figure 1 shows.

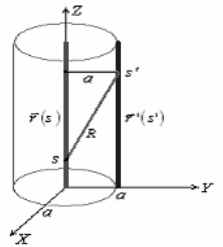

Figure 1. Geometry for the straight wire.

As shown in figure 2, general geometries require a model encompassing the bent characteristics. This model is given by the general Pocklington equation [1, 4], formally obtained from Maxwell equations, magnetic and electric potentials and Lorenz's gauge [5]:

$$E_{\tan}^{i} = -\frac{j}{\omega\varepsilon}\int_{s'} I_s(s')\left[k^2\mathbf{s}\bullet\mathbf{s}' + \frac{\partial^2}{\partial s\partial s'}\right]\frac{e^{-jkR}}{4\pi R}ds'. \qquad (1)$$

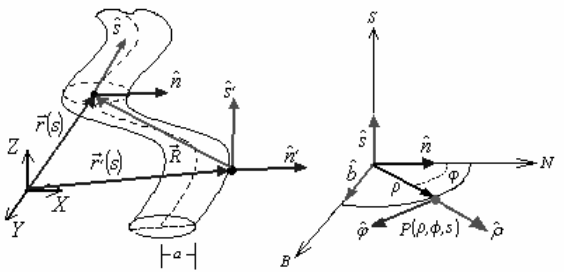

Figure 2. Arbitrary bent wire and relations between its vectors and its geometry.

According to figure 2, a small wire's segment defines a local co-ordinate system, rotated around the reference co-ordinate system. Such rotation is represented by $\mathbf{s} \bullet \mathbf{s}'$, and the antenna geometry is defined by $\mathbf{s}(s)$, $\mathbf{r}(s)$, $\mathbf{s}'(s')$ and $\mathbf{r}'(s')$.

The general Pocklington equation can be simplified, in order to obtain a more efficient solution, by expanding the integral kernel using the vectorial equation that represents the wire's axis, and the equivalent current filament equation, related to co-ordinate system, expressed as:

$$\mathbf{r}(s) = x(s)\mathbf{i} + y(s)\mathbf{j} + z(s)\mathbf{k}\,, \quad \mathbf{r}'(s') = \mathbf{r}(s') + a\mathbf{n}(s')\,, \qquad (2)$$

where $\mathbf{n}(s)$ is the unit normal vector for the wire's axis. As seen, the curve representing the current filament is a parallel curve to the one representing the wire's axis. For any particular antenna geometry, it is possible to define the tangential unit vectors to obtain the dot product $\mathbf{s} \bullet \mathbf{s}'$ defined by:

$$\begin{aligned} \mathbf{s}(s) &= \frac{dx(s)}{ds}\mathbf{i} + \frac{dy(s)}{ds}\mathbf{j} + \frac{dz(s)}{ds}\mathbf{k}\,, \\ \mathbf{s}'(s') &= \frac{dx'(s')}{ds'}\mathbf{i} + \frac{dy'(s')}{ds'}\mathbf{j} + \frac{dz'(s')}{ds'}\mathbf{k}\,. \end{aligned} \qquad (3)$$

Once the vectorial relationship has been found, it is possible to simplify the kernel of (1) expanding the operator $\partial^2 / \partial s \partial s'$ over the Green's functions, as it is shown in the following:

$$\left[k^2\mathbf{s}\bullet\mathbf{s}'+\frac{\partial^2}{\partial s\partial s'}\right]\frac{e^{-jkR}}{4\pi R}=$$

$$\left[R^2\left(k^2R^2-1-jkR\right)\mathbf{s}\bullet\mathbf{s}'+\left(3+3jkR-k^2R^2\right)(\mathbf{R}\bullet\mathbf{s})(\mathbf{R}\bullet\mathbf{s}')\right]\frac{e^{-jkR}}{4\pi R^5},$$

$$R=|\mathbf{R}|=|\mathbf{r}-\mathbf{r}'|=\sqrt{[x(s)-x'(s')]^2+[y(s)-y'(s')]^2+[z(s)-z'(s')]^2}\ , \quad (4)$$

where R is the distance between the observation and source points. Since the parallel curve is at a distance from the axis curve, the analysis points never coincide. Thus, there are no singularities. After applying (4), equation (1) is transformed into a pure integral equation:

$$E^i_{\tan}=-\frac{j}{\omega\varepsilon}$$

$$\int_{s'}I_s(s')\left[R^2\left(k^2R^2-1-jkR\right)\mathbf{s}\bullet\mathbf{s}'+\left(3+3jkR-k^2R^2\right)(\mathbf{R}\bullet\mathbf{s})(\mathbf{R}\bullet\mathbf{s}')\right]\frac{e^{-jkR}}{4\pi R^5}ds'. \quad (5)$$

In the case of a straight antenna, as in figure 1, equation (5) is transformed into the well- known integral relation found in the applied literature [6]:

$$E^i_{\tan}=\frac{j}{\omega\varepsilon}\int_{s'}I_s(s')\left[(1+jkR)\left(2R^2-3a^2\right)+k^2a^2R^2\right]\frac{e^{-jkR}}{4\pi R^5}ds', \quad (6)$$

We solve equation (5) with the MM that applies the point-matching technique [7], using pulse functions as basis functions $i_n(s')$ and Dirac's delta functions as weight functions $w_m(s)$.

$$i_n(s')=\begin{cases}1 & \text{if} \quad (n-1)\Delta s'\le s'<n\Delta s'\\ 0 & \text{elsewhere}\end{cases},$$

$$w_m=\delta(s-s_m), \quad m,n=1,2,\cdots,N\ . \quad (7)$$

The general MM for the antenna matrix equation is given by:

$$\left[Z_{mn}\right]\left(I_n\right)=\left(V_m\right), \tag{8}$$

where $\left[Z_{mn}\right]$ is known as the impedance matrix, given by:

$$Z_{mn}=$$

$$-\frac{j}{4\pi\omega\varepsilon}\int_{(n-1)\Delta s'}^{n\Delta s'}\left[R^2\left(k^2R^2-1-jkR\right)\mathbf{s}\bullet\mathbf{s}'+\left(3+3jkR-k^2R^2\right)\left(\mathbf{R}\bullet\mathbf{s}\right)\left(\mathbf{R}\bullet\mathbf{s}'\right)\right]\frac{e^{-jkR}}{R^5}ds'\Bigg|_{s=s_m}, \tag{9}$$

while $\left(V_m\right)$ matrix, known as voltage matrix, is determined by:

$$V_m=\int_s w_m E^i_{\tan}ds\,, \tag{10}$$

and $\left(I_n\right)$ matrix, known as current matrix, is:

$$\left(I_n\right)=\left[Z_{mn}\right]^{-1}\left(V_m\right), \tag{11}$$

Champagne et al formulation

Champagne's approach expresses the electric field in terms of the magnetic vector potential $\mathbf{A}\left(\mathbf{r}\right)$ and electric scalar potential $\Phi\left(\mathbf{r}\right)$:

$$-\mathbf{E}^i_{\tan}\left(\mathbf{r}\right)=-\left[\,j\omega\mathbf{A}\left(\mathbf{r}\right)+\nabla\Phi\left(\mathbf{r}\right)\right]_{\tan}, \qquad \mathbf{r} \quad \text{on} \quad S\,, \tag{12}$$

where $\mathbf{E}^i_{\tan}$ is the tangential impressed electric field on the wire's surface represented by S, and:

$$\mathbf{A}(\mathbf{r}) = \frac{\mu}{4\pi}\int_S \frac{\mathbf{I}(\mathbf{r}')}{2\pi a(\mathbf{r}')}\frac{e^{-jkR}}{R}dS',$$
$$\Phi(\mathbf{r}) = -\frac{1}{j4\pi\omega\varepsilon}\int_S \nabla'_S \bullet \left(\frac{\mathbf{I}(\mathbf{r}')}{2\pi a(\mathbf{r}')}\right)\frac{e^{-jkR}}{R}dS', \quad (13)$$

R is the distance between the source and observation points. When applying MM, the total current $\mathbf{I}(\mathbf{r})$ is approximated by a series of independent piecewise linear expansion functions $\mathbf{\Lambda}_n(\mathbf{r})$ such:

$$\mathbf{I}(\mathbf{r}) \approx \sum_{n=1}^{N} I_n \mathbf{\Lambda}_n(\mathbf{r}), \quad (14)$$

The I_n's are unknown current coefficients and N is the total number of unknowns. In this way, the potentials are expressed by expansion series as follows:

$$\mathbf{A}(\mathbf{r}) = \sum_{n=1}^{N} I_n \mathbf{A}_n(\mathbf{r}), \quad \Phi(\mathbf{r}) = \sum_{n=1}^{N} I_n \Phi_n(\mathbf{r}), \quad (15)$$

Using (14) and (15) in (13), potentials are defined as:

$$\mathbf{A}_n(\mathbf{r}) = \frac{\mu}{4\pi}\int_{\sigma_{n-1}}^{\sigma_{n+1}} \frac{1}{2\pi}\int_{-\pi}^{\pi} \mathbf{\Lambda}_n(\mathbf{r}')\frac{e^{-jkR}}{R}d\varphi' d\sigma',$$
$$\Phi_n(\mathbf{r}) = -\frac{1}{j4\pi\omega\varepsilon}\int_{\sigma_{n-1}}^{\sigma_{n+1}} \frac{1}{2\pi}\int_{-\pi}^{\pi} \nabla'_S \bullet \mathbf{\Lambda}_n(\mathbf{r}')\frac{e^{-jkR}}{R}d\varphi' d\sigma'. \quad (16)$$

Potential equations perform integrations along the arc length σ and around the perimeter φ. Notice that these integrals consider any wire's radius, then the kernel functions are singular when the observation point coincides with the source one. Champagne avoids the problem in solving singularities apart by approximation and

adding the non- singular solution. In spite of its generality, this procedure complicates more the solution. The basis and weight function chosen by Champagne et al is given by:

$$\mathbf{\Lambda}_n(\mathbf{r}) = \begin{cases} \mathbf{\Lambda}_n^+(\mathbf{r}) = \xi \hat{l}_{n^+}(\xi), & \mathbf{r} \quad \text{in} \quad S_{n^+} \\ \mathbf{\Lambda}_n^-(\mathbf{r}) = (1-\xi)\hat{l}_{n^-}(\xi), & \mathbf{r} \quad \text{in} \quad S_{n^-} \\ 0, & \text{otherwise} \end{cases} \tag{17}$$

where ξ is a normalized variable which performs the transformation $\sigma \in [\sigma_{n-1}, \sigma_n] \to \xi[0,1]$. The plus and minus signs, identify the positive or negative slope of the segment.

The circular loop antenna for the Pocklington general equation.

The circular loop antenna of figure 3 is characterized by the following equations:

$$\begin{aligned} &\mathbf{r}(s) = A\cos\left(\frac{s}{A}\right)\mathbf{i} + Asen\left(\frac{s}{A}\right)\mathbf{j}, \quad \mathbf{s}(s) = -\sin\left(\frac{s}{A}\right)\mathbf{i} + \cos\left(\frac{s}{A}\right)\mathbf{j}, \\ &\mathbf{r}'(s') = \mathbf{r}(s') + a\mathbf{k}, \quad \mathbf{s}'(s') = -\sin\left(\frac{s'}{A}\right)\mathbf{i} + \cos\left(\frac{s'}{A}\right)\mathbf{j}, \end{aligned} \tag{18}$$

where A is the antenna's radius and a is the wire's radius.

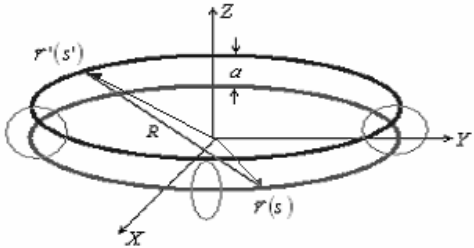

Figure 3. Circular loop antenna and its associated vectors.

The loop is fed by a unit delta gap source located at $\varphi = 0^{o}$ and has the following parameters:

$f = 3\,GHz$, $N = 17$ segments, $A = 0.0637\lambda$, $a = 0.0027\lambda$.

Figure 4 shows the real and imaginary parts of the current distribution, from which we can make comparisons to the Champagne technique [2]. The results we have chosen to compare are those of the eight quadratic segments with a four-point Gaussian quadrature numerical scheme (4-pt GQ). This is remarkable if we consider to use a numerical integral scheme based on the Simpson rule. As we can see, there is an uniform error of 5% in the whole current distribution; for practical uses, it will be neglected.

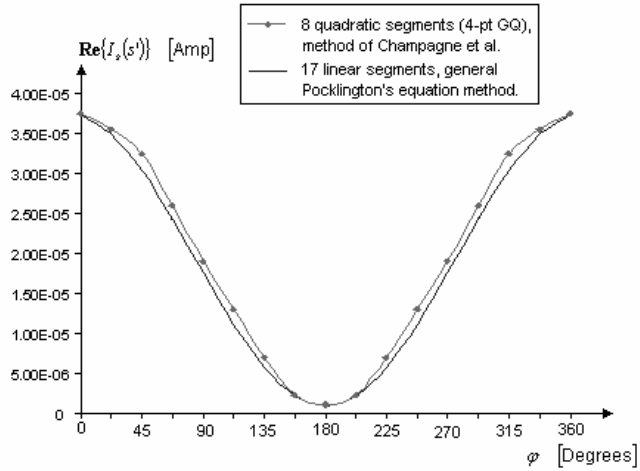

Figure 4a. Real component current distribution

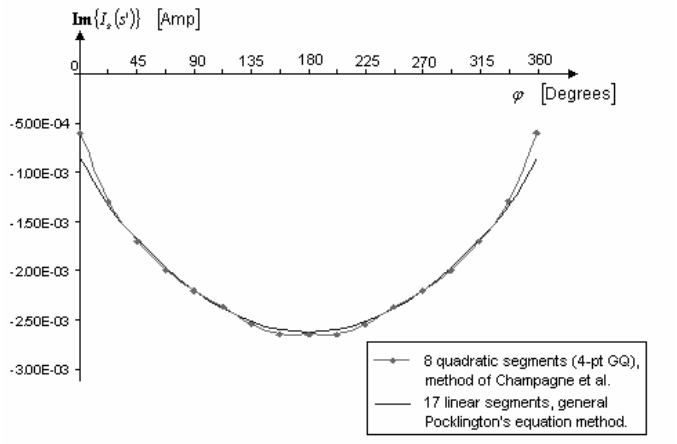

Figure 4b Imaginary component current distribution

Computational comparison

Champagne et al. and Pocklington methods were programmed by using a Visual C++ 6.0 compiler. This allows to create 32 bits applications for shell environments and for GUI environments as well. Both methods were developed as shell applications and the current distribution results were plotted in another graphical program.

Both programs use libraries for handling complex numbers, matrices and vectors. In Visual C++ 6.0, each matrix element consists of a 16 bytes register. This is due to the fact that each complex number is performed by two real numbers with double data type. In this compiler version, 8 bytes are necessary for storage each of *double* register. In this way for both methods, the amount of memory for the matrices is

$$\left.\begin{array}{l}\text{Memory for } [Z_{mn}] = 16N^2 \text{ Bytes} \\ \text{Memory for } [V_m] = 16N \text{ Bytes} \\ \text{Memory for } [I_n] = 16N \text{ Bytes}\end{array}\right\} \text{ Total memory} = 16\left(2N + N^2\right)$$

In the Champagne method, which uses 8 segments the amount of used memory is:

$$\text{Total memory} = 16\left(2\times 8 + 8^2\right) = 16\left(16 + 64\right) = 1280 \text{ Bytes} = 1.25 \text{ MBytes}$$

where as in the Pocklington method, which uses 17 segments, the total amount of used memory is:

$$\text{Total memory} = 16\left(2\times 17 + 17^2\right) = 16\left(34 + 289\right) = 5168 \text{ Bytes} = 5.04 \text{ MBytes}$$

It is clear that in the Champagne method the amount of used memory is less than in the Pocklington method. This is because

Champagne uses fewer segments than Pocklington does. However if both use the same number of segments, the amount of used memory is the same in each case.

Due to its generality, the Champagne method evaluates several integrals numerically. This is seen in the fact that it takes into account any wire's radius and the use of Galerkin technique. Thus number of performed integrations is:

$$\text{Number of integrations in } \left[Z_{mn}\right] = \text{Number of integrations in } \left[Z_{mn}^{A}\right] + \text{Nur}$$
$$= 6N^2 + 4N^2 = 10N^2$$

$$\text{Number of integrations in } \left[V_m\right] = 2N$$

$$\text{Total of integrations} = 2N + 10N^2 = 2 \times 7 + 10 \times 49 = 504$$

In Pocklington method, the number of performed integrations is:

$$\text{Number of integrations in } \left[Z_{mn}\right] = N^2$$

$$\text{Number of integrations in } \left[V_m\right] = N$$

$$\text{Total of integrations} = N + N^2 = 17 + 17^2 = 306$$

Therefore, since Pocklington method performs fewer integrations, it is more rapid than Champagne's one. Differences would be more pronounced if Champagne would have used the same number of segments than Pocklington did. In that case, the results are the following:

$$\text{Total of integrations} = 2N + 10N^2 = 2 \times 17 + 10 \times 289 = 2924$$

$$\text{Total memory} = 16\left(2N + N^2\right) = 16\left(34 + 289\right) = 5168 \text{ Bytes} = 5.04 \text{ MByte}$$

Conclusion

This paper tries to apply the Pocklington equation results to the circular loop antenna. If, for practical uses, an error of 5 % is neglected, Pocklington results are similar to those of Champagne's formulation. The difference between both procedures is that we use the very simple point-matching technique and the Simpson's rule for integration, where as Champagne uses the Galerkin method and the Gaussian quadrature technique for integration.

Although Champagne et al consider any thickness for the wire's antenna, in practice, most of the antennas are thin in comparison to the wave-length of the electromagnetic field. Thus, an appropriate model for such antennas would be the general Pocklington equation. By emphatizing the vectorial representation for modeling the wire, we got a formulation which can be used for linear or curved antennas. We conclude then that the proposed model represents correctly the electromagnetic antenna's behavior for an arbitrary geometry [1, 4, 6].

References

[1] Barrera-Figueroa, V., Sosa-Pedroza, J. and López-Bonilla, J. Simplification of Pocklington integral equation for arbitrary bent thin wires, Boundary Elements XXVII edition, (Electrical Engineering and Electromagnetics), Eds. A. Kassab, C. A. Brebbia, E. Divo and D. Poljak. WIT Trans. on Modelling and Simulation, WIT Press, vol. 39, pp. 563-574, 2005.

[2] Champagne J., Nathan II, T. Williams, Jeffery and R. Wilton, Donald, The use of curved segments for numerically modelling thin wire antennas and scatterers, IEEE Trans. on Antennas and Propagation, vol. 40, No. 6, p.p. 682-689, June 1992.

[3] Mei, K. K., On the integral equations of thin wire antennas, IEEE Trans. on Antennas and Propagation, vol. AP-13, pp 374-378, 1965,.

[4] Tang, C. H., Input impedance of arc antennas and short helical radiators, IEEE Trans. on Antennas and Propagation, vol. AP-12, pp 2-9, 1963.

[5] Sosa- Pedroza, J., López-Bonilla, J. and Barrera-Figueroa, V. "La ecuación generalizada de Pocklington para antenas de alambre de forma arbitraria"; Revista Científica (The Mexican Journal of Electromechanical Engineering) ESIME-IPN vol 9, N.2, pp 83-86, 2005

[6] Stutzman, W.L. and Thiele, G.A. Antenna, theory and design, p. 488, chap. 10. Ed. John Wiley & Sons, New York,1998.

[7] Werner, D. H., Werner, P. L. and Breakall, J. K. Some computational aspects of Pocklington electric field integral equation for thin wires, IEEE Trans. on Antennas and Propagation, Vol. 42, No. 4, pp. 561-563, 1994.